

## The Aerosol Radiative Effect on a Severe Haze Episode in the Yangtze River Delta

Kai SUN<sup>1</sup>, Hongnian LIU<sup>1\*</sup>, Xueyuan WANG<sup>1</sup>, Zhen PENG<sup>1</sup>, and Zhe XIONG<sup>2</sup>

<sup>1</sup> School of Atmospheric Sciences, Nanjing University, Nanjing 210023

<sup>2</sup> Key Laboratory of Climate-Environment for East Asia, Institute of Atmospheric Physics, Chinese Academy of Sciences, Beijing 100029

(Received January 22, 2017; in final form June 14, 2017)

### ABSTRACT

Due to increased aerosol emissions and unfavorable weather conditions, severe haze events have occurred frequently in China in the last 10 years. In addition, the interaction between the boundary layer and the aerosol radiative effect may be another important factor in haze formation. To better understand the effect of this interaction, the aerosol radiative effect on a severe haze episode that took place in December 2013 was investigated by using two WRF-Chem model simulations with different aerosol configurations. The results showed that the maximal reduction of regional average surface shortwave radiation, latent heat, and sensible heat during this event were 88, 12, and 37 W m<sup>-2</sup>, respectively. The planetary boundary layer height, daytime temperature, and wind speed dropped by 276 m, 1°C, and 0.33 m s<sup>-1</sup>, respectively. The ventilation coefficient dropped by 8%–24% for in the central and northwestern Yangtze River Delta (YRD). The upper level of the atmosphere was warmed and the lower level was cooled, which stabilized the stratification. In a word, the dispersion ability of the atmosphere was weakened due to the aerosol radiative feedback. Additional results showed that the PM<sub>2.5</sub> concentration in the central and northwestern YRD increased by 6–18 µg m<sup>-3</sup>, which is less than 15% of the average PM<sub>2.5</sub> concentration during the severely polluted period in this area. The vertical profile showed that the PM<sub>2.5</sub> and PM<sub>10</sub> concentrations increased below 950 hPa, with a maximum increase of 7 and 8 µg m<sup>-3</sup>, respectively. Concentrations reduced between 950 and 800 hPa, however, with a maximum reduction of 3.5 and 4.5 µg m<sup>-3</sup>, respectively. Generally, the aerosol radiative effect aggravated the level of pollution, but the effect was limited, and this haze event was mainly caused by the stagnant meteorological conditions. The interaction between the boundary layer and the aerosol radiative effect may have been less important than the large-scale static weather conditions for the formation of this haze episode.

**Key words:** haze, aerosol radiative effect, Yangtze River Delta, ventilation coefficient, PM<sub>2.5</sub>, WRF-Chem

**Citation:** Sun, K., H. N. Liu, X. Y. Wang, et al., 2017: The aerosol radiative effect on a severe haze episode in the Yangtze River Delta. *J. Meteor. Res.*, **31**(5), 865–873, doi: 10.1007/s13351-017-7007-4.

## 1. Introduction

Aerosols affect the climate by influencing the energy budget of the earth. This is referred to as the climate effect of aerosols, and many relevant works have been conducted to study this effect (IPCC, 2007; Forkel et al., 2012; Zhao and Garrett, 2015). In the last 10 years, haze events have occurred frequently in China, with extreme aerosol concentrations usually reaching above 200 µg m<sup>-3</sup> (Tie and Cao, 2009; Tao et al., 2014; Zhang L. et al., 2015). The influences on meteorological fields imposed by the high concentrations of aerosols during haze events are quite different from those reported by relevant stud-

ies focusing on longer time periods, such as one year, which are generally accompanied by lower aerosol concentrations. Firstly, the influences of aerosols on meteorological factors during haze events are obvious. Zhang B. et al. (2015) analyzed a severe haze event in China during January 2013 and found that the surface downward shortwave radiation, 2-m temperature, 10-m wind speed, and planetary boundary layer (PBL) height decreased by 84.0 W m<sup>-2</sup>, 3.2°C, 0.8 m s<sup>-1</sup>, and 268 m, respectively. Secondly, changes in meteorological factors during haze events are temporary, and fluctuate widely with variations in pollutant concentrations.

The interaction between high concentrations of aero-

Supported by the National Key Research and Development (973) Program (2014CB441203), National Natural Science Foundation of China (41575141 and 41305006), and Collaborative Innovation Center of Climate Change in Jiangsu Province.

\*Corresponding author: liuhn@nju.edu.cn.

©The Chinese Meteorological Society and Springer-Verlag Berlin Heidelberg 2017

sols and meteorological fields during haze events mainly include: (i) the changes in meteorological factors such as temperature, wind fields, and PBL height due to aerosol radiative effects, which in turn affect the transport and diffusion of the aerosols themselves (Ding et al., 2013; Yang et al., 2015); and (ii) the attenuation of incoming solar radiation, which affects the photochemical processes of pollutants (Wendisch et al., 2010; Zhang et al., 2010). To date, whilst we have a general understanding of the mechanism involved in the interaction between aerosols and meteorological factors, the specific degree of interaction still needs to be more thoroughly investigated. In particular, how this interaction increases pollutant concentrations during heavy haze events, which then further aggravates the level of pollution, is not well understood. Additionally, relevant findings can effectively improve the accuracy of air quality forecasts (Wang et al., 2013, 2014; Zhang et al., 2014). Therefore, in this study, we selected and simulated a severe haze event that occurred in early December 2013 in the Yangtze River Delta (YRD) to analyze the aerosol radiative effect during various periods of this pollution event.

## 2. Methodology and data

### 2.1 Model configuration

Version 3.5.1 of WRF-Chem (Grell et al., 2005) was used for the simulation in this study. The major physics options selected included the Goddard shortwave radiation scheme, the Rapid Radiative Transfer Model longwave radiation scheme (Mlawer et al., 1997), the Fast-J photolysis scheme (Wild et al., 2000), the Noah land-surface module (Chen and Dudhia, 2001), the Yonsei University PBL scheme (Hong et al., 2006), the WRF single moment 5-class cloud microphysics (Hong et al., 2004), and the Grell 3D cumulus parameterization. The gas-phase chemical mechanism adopted was the Regional Acid Deposition Model, version 2 (Stockwell et al., 1990). The modal aerosol dynamics model for Europe (Ackermann et al., 1998) and the secondary organic aerosol model (Schell et al., 2001) were used for the aerosols. For the calculation of biogenic emissions, the model of emissions of gases and aerosols from nature (Guenther et al., 2006) was adopted. For land use, the 1-km moderate resolution imaging spectroradiometer data (Friedl et al., 2002) were employed.

The initial and boundary meteorological conditions were obtained from the NCEP global final (FNL) analysis data, available every 6 h at a grid spacing of  $1^\circ \times 1^\circ$ . The chemical initial and boundary conditions were obtained

from simulations of the model for ozone and related chemical tracers, version 4, at a resolution of  $1.9^\circ \times 2.5^\circ$  (Emmons et al., 2010).

The model adopts three layers of nesting, and the grid resolutions of the outermost (D01), middle (D02), and innermost (D03) layers were  $27 \text{ km} \times 27 \text{ km}$ ,  $9 \text{ km} \times 9 \text{ km}$ , and  $3 \text{ km} \times 3 \text{ km}$ , respectively. The D03 layer covered the entire YRD, and the number of grid points was 241 (east–west)  $\times$  265 (south–north). The model includes a total of 25 vertical levels, and the pressure at the top of the model was set to 50 hPa. The simulation was initiated at 0000 UTC 27 November 2013 and ended at 0000 UTC 12 December 2013, with data outputted hourly. The first 24 hours of the simulation were discarded as model spin-up time, and thus we began the analysis at 0000 UTC 28 November 2013. A total of 14 days of results were analyzed.

Two experiments were carried out. In the first experiment (Case-1), all aerosol feedbacks were completely switched off; whereas, in the second experiment (Case-2), the direct aerosol radiative effect was included. To compute the optical characteristics of aerosols in Case-2, we used the volume approximation scheme. Except for the difference mentioned above, the other model settings in Case-2 remained the same as in Case-1. The differences between the two sets of simulation results (i.e., Case-2 minus Case-1) were used to identify the influence of the aerosol direct radiative effect on meteorological factors.

An evaluation of the Case-1 simulation against observational data, together with some further analysis of this episode, such as its formation and dissipation processes, the chemical composition of the fine particles, and the pollutants' spatial distribution, is detailed in another paper (Sun et al., 2016).

### 2.2 Anthropogenic emissions

In this study, we obtained information on anthropogenic emissions from the Multi-resolution Emission Inventory for China (MEIC; <http://www.meicmodel.org>; He, 2012), and allocated it vertically in the model using the method of Wang et al. (2010). MEIC is a newly released emissions inventory for China, and its horizontal resolution is  $0.25^\circ \times 0.25^\circ$ . It includes emissions information on black carbon, CO,  $\text{CO}_2$ ,  $\text{NH}_3$ ,  $\text{NO}_x$ , organic carbon,  $\text{PM}_{2.5}$ ,  $\text{PM}_{10}$ ,  $\text{SO}_2$ , and non-methane volatile organic compounds for five sectors (power, industry, residential, transportation, and agriculture). MEIC was developed by the INTEX-B (Intercontinental Chemical Transport Experiment) team at Tsinghua University of China.

### 3. Results

#### 3.1 Characteristics of the haze episode

We divided the haze event into three periods: Phases 1, 2, and 3, corresponding to the pre-pollution period (0000 UTC 28 to 2300 UTC 30 November), the severely polluted period (0000 UTC 1 to 2300 UTC 8 December), and the post-pollution period (0000 UTC 9 to 2300 UTC 11 December).

Figure 1 shows the spatial distribution of the average  $\text{PM}_{2.5}$  concentration in Phase 2. It shows that the  $\text{PM}_{2.5}$  concentration was high in the central and northwestern YRD. The average  $\text{PM}_{2.5}$  concentration of the urban agglomeration (Nanjing–Suzhou–Shanghai) in the central area of the YRD exceeded  $220 \mu\text{g m}^{-3}$ . The surrounding area of Hefei City, Anhui Province, was also a center of high  $\text{PM}_{2.5}$  concentration ( $> 220 \mu\text{g m}^{-3}$ ), whereas the value was generally above  $160 \mu\text{g m}^{-3}$  in the vast area of the northwestern YRD (Jiangsu Province and the northern part of Anhui Province).

#### 3.2 Influence of the aerosol radiative effect on meteorological factors

Figure 2 shows the influence of the aerosol radiative effect on the mean meteorological factors and  $\text{PM}_{2.5}$  concentration during Phase 2. For radiative factors, it shows that there was a considerable reduction in the average

downward shortwave radiation in the whole of the YRD (Fig. 2a). The surface shortwave radiation in the central YRD decreased by  $52\text{--}65 \text{ W m}^{-2}$ . This was the region with the largest reduction, although there was also a marked reduction in the northwestern YRD ( $39\text{--}65 \text{ W m}^{-2}$ ). The sensible heat decreased over the land area of the YRD, and in particular, the maximum reduction in the central YRD exceeded  $12 \text{ W m}^{-2}$  (Fig. 2b). The latent heat also reduced in the YRD, and it decreased by  $2\text{--}4 \text{ W m}^{-2}$  in the central and northwestern areas of the YRD (Fig. 2c). The surface shortwave radiation decreased obviously in the region of high  $\text{PM}_{2.5}$  concentration, which indicates that the aerosol radiative effect attenuated the shortwave solar radiation that reached the ground surface. For temperature, in the central and northwestern YRD, where the reduction in incident shortwave radiation was large, both the daytime and nighttime ground surface temperature decreased (Figs. 2e, f). Moreover, the reduction in temperature was more severe during the day than at nighttime, which resulted from the daytime temperature having a stronger relationship with the incident shortwave solar radiation and, at night, atmospheric aerosols reflecting the upward longwave radiation from the ground surface, causing a warming effect on the near-surface atmosphere. The decrease in temperature also caused the PBL height to reduce by 80 m (Fig. 2d). The influence of the aerosol radiative effect on the near-surface wind speed was relatively small, with the maximal decrease reaching  $0.15 \text{ m s}^{-1}$ . As for relative humidity, it increased by 1%–4% due to the aerosol radiative effect.

Figure 3 shows the time series for the influence of the aerosol radiative effect on the regional average results, and the selected region is north of  $29.5^\circ\text{N}$  in the innermost domain. We can see that, during Phase 2, the downward shortwave radiation, latent heat flux, and sensible heat flux decreased considerably. During 6–7 December, when the aerosol concentration reached its maximum, the downward shortwave radiation, latent heat flux, and sensible heat flux decreased by  $88$ ,  $12$ , and  $37 \text{ W m}^{-2}$ , respectively. Moreover, the daytime temperature decreased by  $1^\circ\text{C}$  on 7 December; the boundary layer height decreased by 276 and 263 m on 3 and 6 December, respectively; and the wind speed decreased by  $0.33 \text{ m s}^{-1}$  on 8 December. From Fig. 3d, we can see that the wind speed did not vary so closely with the aerosol concentration as other meteorological factors. Generally, the aerosol radiative effect during this haze event caused radiative factors (e.g., surface shortwave radiation, latent heat flux, and sensible heat flux) to decrease, and thus the temperature decreased as a result. The reduction in

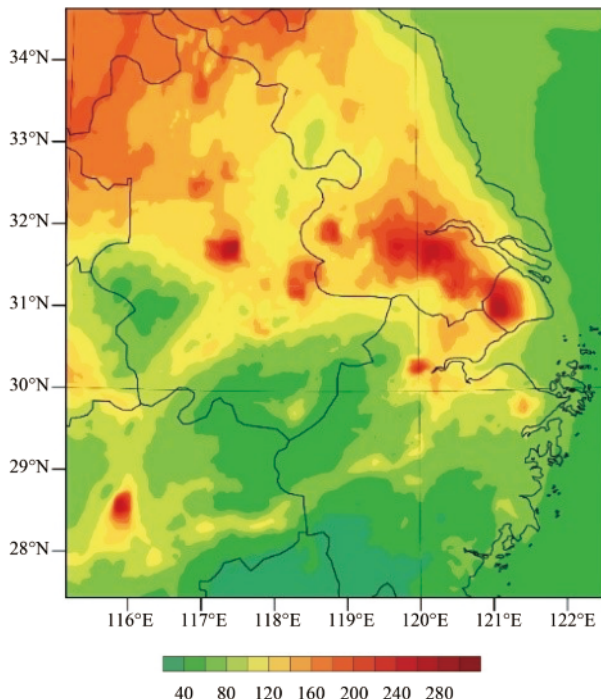


**Fig. 1.** Simulated average surface  $\text{PM}_{2.5}$  concentration ( $\mu\text{g m}^{-3}$ ) during the severely polluted period.

PBL height and wind speed weakened the ability of the atmosphere to diffuse and dilute pollutants.

Figure 4 shows the rate of change (%) in the average ventilation coefficient (VC) due to the aerosol radiative effect during Phase 2. The VC was defined in Sun et al. (2016), and is an indicator of the horizontal dispersion ability of the atmosphere. The lower the VC is, the weaker the ability of the atmosphere has to disperse pollutants horizontally. From Fig. 4, we can see that the VC decreased throughout almost the whole of the YRD, and the reduction in the central and northwestern YRD varied

between 8% and 24%, which may have been mainly due to the reduced near-surface wind speed and PBL height.

Figure 5 compares the average vertical temperature profile at Nanjing ( $32.12^{\circ}\text{N}$ ,  $118.95^{\circ}\text{E}$ ) for the two cases. We can see that the temperature of the lower atmosphere decreased, but that of the upper layer increased. This was because the aerosol radiative effect cooled the lower atmosphere and warmed the upper layer via the scattering and absorption effects of aerosols. Generally, the radiative forcing at the surface and the top of the atmosphere due to aerosols is negative, and that of an air column is

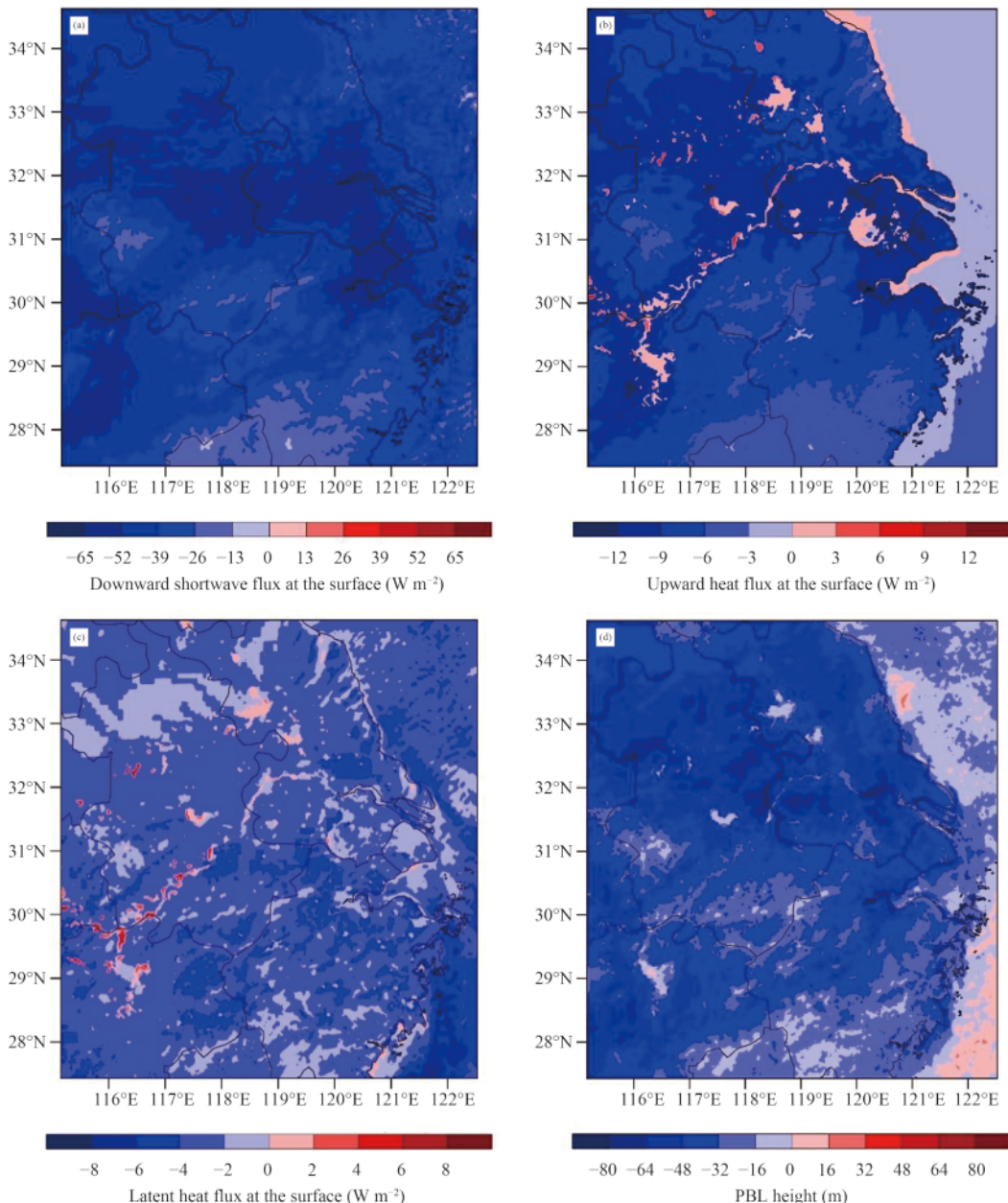


**Fig. 2.** Influence of the aerosol radiative effect on average meteorological factors (Case-2 minus Case-1): (a) downward shortwave radiation at the surface ( $\text{W m}^{-2}$ ); (b) upward sensible heat flux ( $\text{W m}^{-2}$ ); (c) latent heat flux ( $\text{W m}^{-2}$ ); (d) PBL height (m); (e) 2-m nighttime temperature ( $^{\circ}\text{C}$ ); (f) 2-m daytime temperature ( $^{\circ}\text{C}$ ); (g) 2-m relative humidity (%); and (h) 10-m wind speed ( $\text{m s}^{-1}$ ).

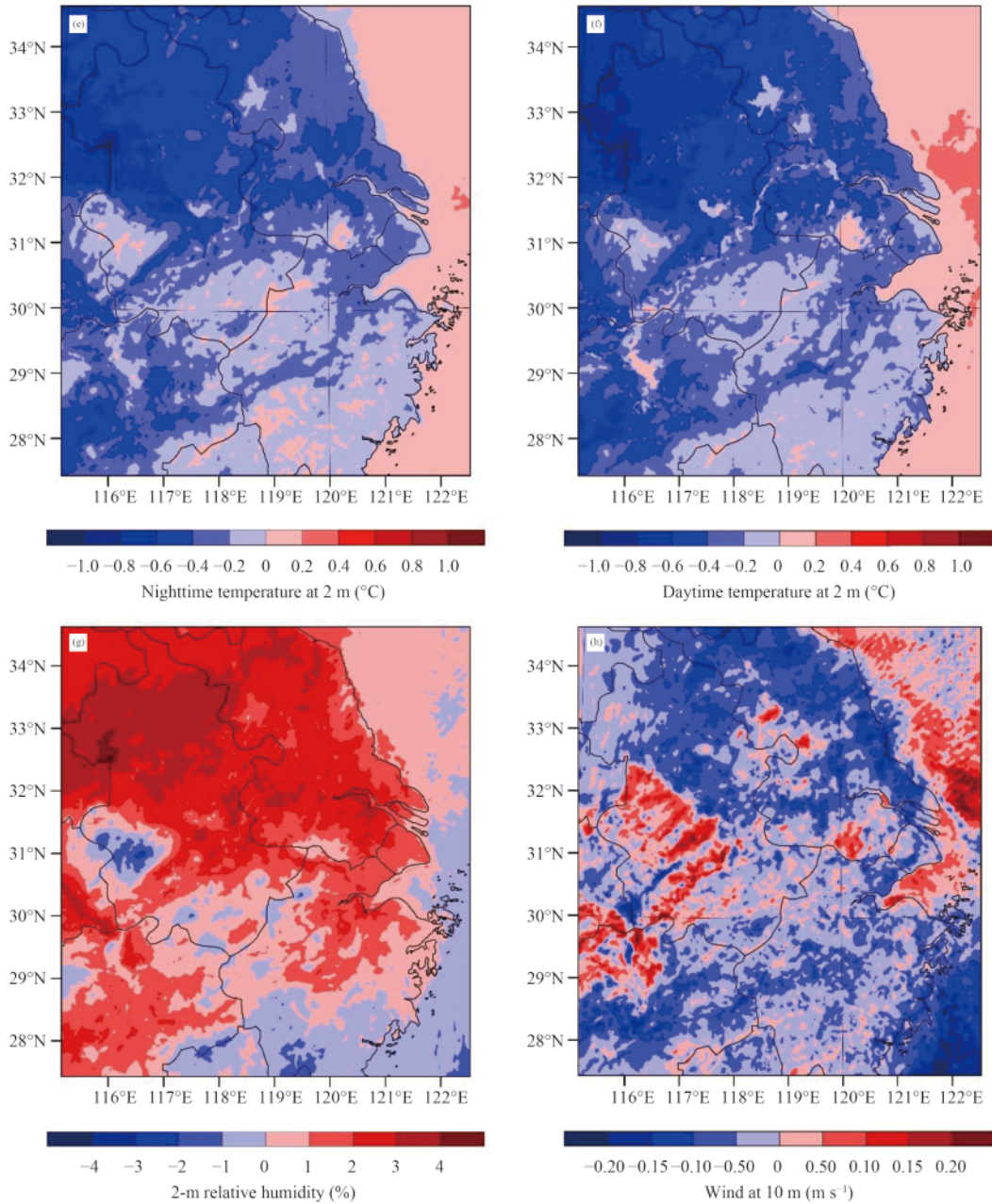


Fig. 2. (Continued).

positive (Liu et al., 2010). In the present case, the effect of warming in the upper layers and cooling in the lower layers further intensified the near-surface temperature inversion shown in Fig. 5, which stabilized the lower atmosphere and thus weakened the vertical transport and diffusion of pollutants.

### 3.3 Influence of the aerosol radiative effect on pollutant concentrations

The weakened horizontal and vertical dispersion ability of the atmosphere, together with high relative humidity, which promotes gas-to-particle transformation, are

important factors in the aggravation of pollution. Figure 6 shows the difference (Case-2 minus Case-1) in the average surface  $\text{PM}_{2.5}$  concentration during Phase 2. From Figs. 4, 6, we can see that, in regions with a large reduction in VC, such as the central and northwestern YRD, the corresponding  $\text{PM}_{2.5}$  concentration increased obviously. Figure 6 shows that, in regions with high  $\text{PM}_{2.5}$  concentrations during the polluted period (e.g., the central YRD; Fig. 1), the  $\text{PM}_{2.5}$  concentration increased by approximately  $6\text{--}24 \mu\text{g m}^{-3}$ . However, in comparison with the original (Case-1) high concentration of  $\text{PM}_{2.5}$  ( $160\text{--}300 \mu\text{g m}^{-3}$ ), the enhancement was no more than

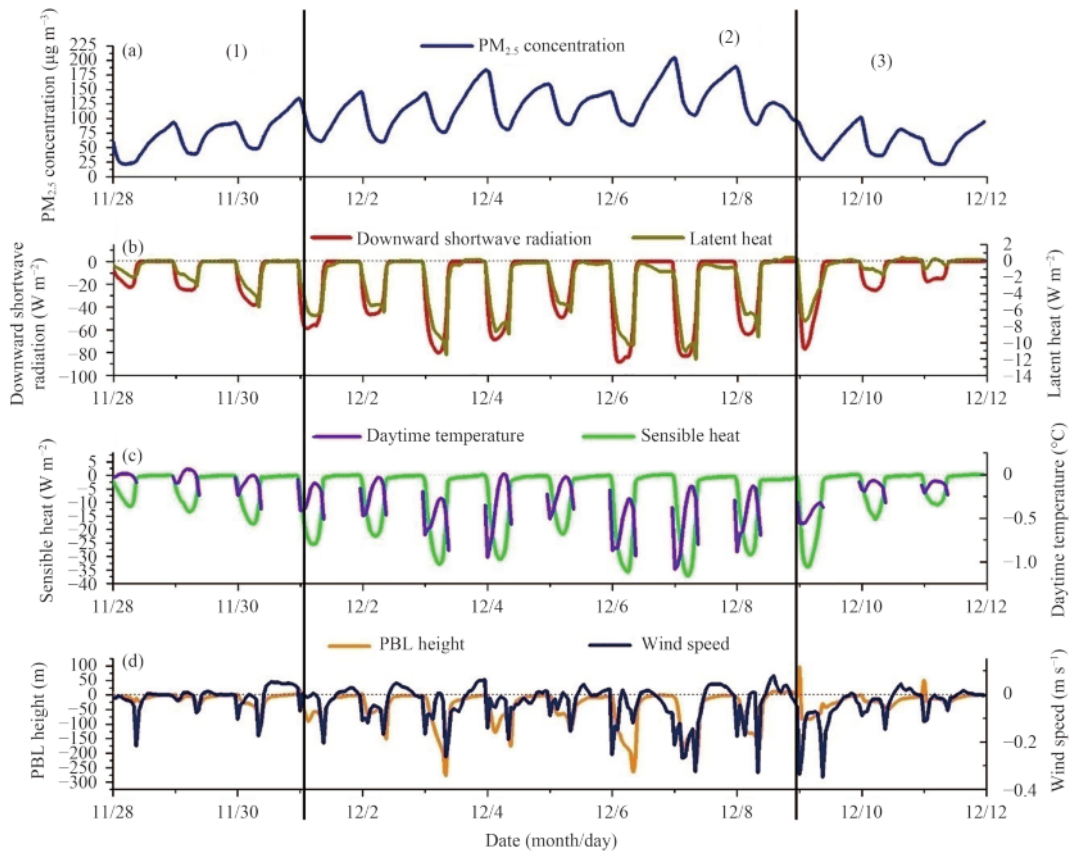


**Fig. 3.** (a) PM<sub>2.5</sub> concentration of Case-1. (b–d) Regional average variations (Case-2 minus Case-1) of meteorological factors caused by the aerosol radiative effect: (b) downward shortwave radiation and latent heat; (c) daytime 2-m temperature and sensible heat; (d) PBL height and 10-m wind speed. The land area to the north of 29.5°N in D03 was selected for the calculations.

15%. We believe that this severe haze event was caused by stagnant meteorological conditions that were not conducive to the dispersion of pollutants. The aerosol radiative effect aggravated the level of pollution, but it was not the determining factor for the formation of this haze event.

Figure 7 shows the influence of the aerosol radiative effect on the vertical profile of the average pollutant concentration in Nanjing. Below approximately 950 hPa, the PM<sub>2.5</sub> and PM<sub>10</sub> concentrations increased by up to 7 and 8  $\mu\text{g m}^{-3}$ , respectively, whereas they decreased by up to 3.5 and 4.5  $\mu\text{g m}^{-3}$  between the levels of 800 and 950 hPa. This probably occurred as the PBL height decreased due to the influence of the aerosol radiative effect, trapping pollutants near the ground surface. In contrast, the O<sub>3</sub> concentration decreased by up to 1.1  $\mu\text{g m}^{-3}$  in the bottom layer of the atmosphere (below 950 hPa), and there was an increase of up to 1.7  $\mu\text{g m}^{-3}$  between the levels of 950 and 770 hPa. This probably occurred because, as the PBL height decreased, aerosols were trapped near the surface. The higher aerosol concentration at the low level reduced the incoming shortwave ra-

diation below 950 hPa and further decreased the O<sub>3</sub> generation rate at this level. On the contrary, at higher levels, with reduced aerosol concentrations, the O<sub>3</sub> concentration increased.

In summary, the aerosol radiative effect weakened the dispersion ability of the atmosphere, which to some extent aggravated the level of aerosol pollution. It also changed the vertical distribution of pollutants, and the influence varied among different kinds of pollutants.

#### 4. Summary

In this study, we used the WRF-Chem model to study the aerosol radiative effect of a severe haze event in the YRD in December 2013. The main conclusions are as follows.

(1) The average PM<sub>2.5</sub> concentration during Phase 2 in the central (Nanjing–Suzhou–Shanghai urban agglomeration) and northwestern YRD exceeded 220 and 160  $\mu\text{g m}^{-3}$ , respectively. The high aerosol concentration reduced the downward shortwave solar radiation reaching the ground surface in the central and northwestern YRD

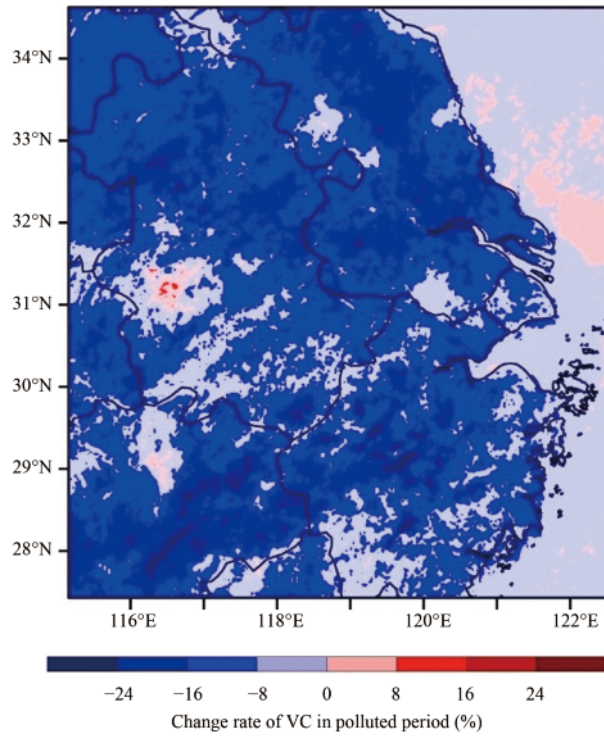


**Fig. 4.** Rate of change (i.e.,  $\frac{\text{Case-2} - \text{Case-1}}{\text{Case-1}} \times 100\%$ ) in the average ventilation coefficient (VC) during Phase 2 due to the aerosol radiative effect.

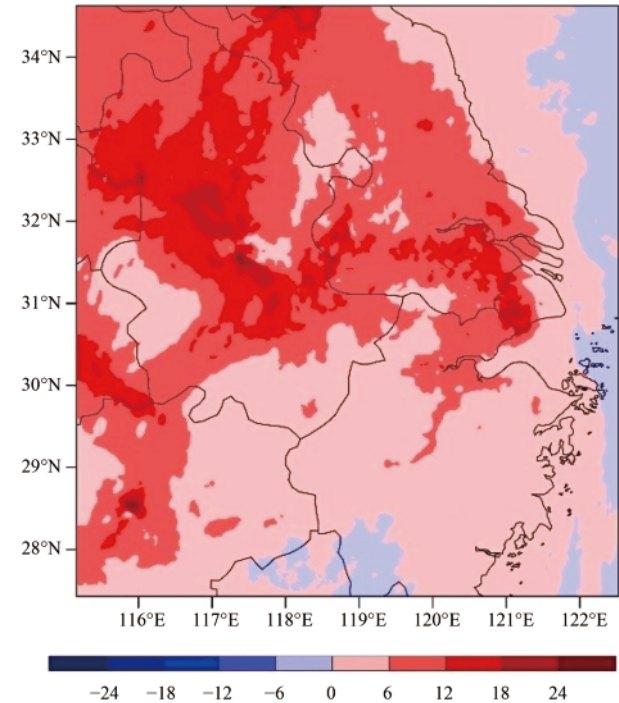


**Fig. 6.** Change (Case-2 minus Case-1) in the average  $\text{PM}_{2.5}$  concentration ( $\mu\text{g m}^{-3}$ ) caused by the aerosol radiative effect during Phase 2.

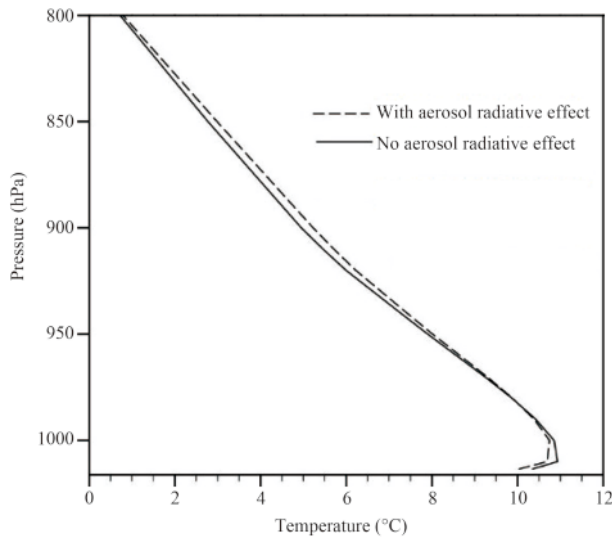


**Fig. 5.** Average temperature profile with (dashed line) and without (solid line) the aerosol radiative effect in Nanjing.

by 52–65 and 39–65  $\text{W m}^{-2}$ , respectively. The daytime and nighttime near-surface temperatures decreased and the cooling effect was more obvious during the day. The maximum reduction in the regional average downward shortwave radiation, latent heat flux, and sensible heat flux was 88, 12, and 37  $\text{W m}^{-2}$ , respectively. During the

daytime, the maximum decreases in temperature, PBL height, and surface wind speed were  $1^\circ\text{C}$ , 276 m, and  $0.33 \text{ m s}^{-1}$ , respectively. The relative humidity increased by 1%–4%.

(2) Due to the reduction in wind speed and boundary layer height, the VC decreased throughout almost the whole of the YRD. The reduction in the VC was 8%–24% in the central and northwestern YRD.

(3) In terms of horizontal dispersion ability, a lower VC was found to result from a lower PBL height and reduced horizontal winds, which indicated that the ability of the atmosphere to transport and diffuse pollutants was weakened. In terms of vertical dispersion ability, the aerosol radiative effect stabilized the lower atmosphere and weakened the vertical dispersion of pollutants, trapping the pollutants near the surface. Consequently, the  $\text{PM}_{2.5}$  concentration in the central and northwestern YRD increased by 6–18  $\mu\text{g m}^{-3}$ —no more than 15% of the average  $\text{PM}_{2.5}$  concentration in Phase 2.

(4) In Nanjing, the  $\text{PM}_{2.5}$  and  $\text{PM}_{10}$  concentrations increased below 950 hPa, with maxima of increase of 7 and 8  $\mu\text{g m}^{-3}$ , respectively, whereas they decreased between 950 and 800 hPa, with maxima of decrease of  $-3.5$  and  $-4.5 \mu\text{g m}^{-3}$ . However, the situation was the opposite for the variation of the  $\text{O}_3$  concentration, which decreased by up to  $1.1 \mu\text{g m}^{-3}$  below 950 hPa and increased by up to  $1.7 \mu\text{g m}^{-3}$  between 950 and 770 hPa. The aerosol radiat-

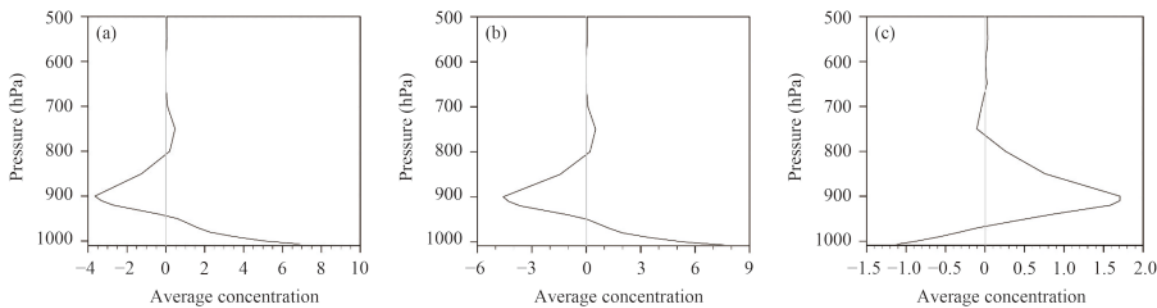


**Fig. 7.** Changes in the average concentration ( $\mu\text{g m}^{-3}$ ) profiles at Nanjing due to the aerosol radiative effect: (a) PM<sub>2.5</sub>, (b) PM<sub>10</sub>, and (c) O<sub>3</sub>.

ive effect changed the vertical distribution of pollutants, and the influence varied among different kinds of pollutants.

This paper reveals that, in the heavy haze event studied, the aerosol radiative effect aggravated the level of pollution to some extent, but was not the determining factor for the formation of the haze. Rather, the stagnant meteorological conditions weakened the dispersion of pollutants and, together with the sustained emission of pollutants, resulted in the high pollutant concentration and the related heavy haze event. Nonetheless, our study demonstrates that, in air quality simulation and forecasting, we should still pay attention to the influence of aerosol radiative feedback.

**Acknowledgments.** The numerical calculations were carried out with the computing facilities at the High Performance Computing Center of Nanjing University. We also acknowledge the free use of MEIC data (<http://www.meicmodel.org>).

## REFERENCES

- Ackermann, I. J., H. Hass, M. Memmesheimer, et al., 1998: Modal aerosol dynamics model for Europe: Development and first applications. *Atmos. Environ.*, **32**, 2981–2999, doi: 10.1016/S1352-2310(98)00006-5.
- Chen, F., and J. Dudhia, 2001: Coupling an advanced land surface hydrology model with the Penn State NCAR MM5 modeling system. Part I: Model implementation and sensitivity. *Mon. Wea. Rev.*, **129**, 569–585, doi: 10.1175/1520-0493(2001)129<0569:CAALSH>2.0.CO;2.
- Ding, A. J., C. B. Fu, X. Q. Yang, et al., 2013: Intense atmospheric pollution modifies weather: A case of mixed biomass burning with fossil fuel combustion pollution in eastern China. *Atmos. Chem. Phys.*, **13**, 10545–10554, doi: 10.5194/acp-13-10545-2013.
- Emmons, L. K., S. Walters, P. G. Hess, et al., 2010: Description and evaluation of the model for ozone and related chemical tracers, version 4 (MOZART-4). *Geosci. Model Dev.*, **3**, 43–67, doi: 10.5194/gmd-3-43-2010.
- Forkel, R., J. Werhahn, A. B. Hansen, et al., 2012: Effect of aerosol–radiation feedback on regional air quality—A case study with WRF/Chem. *Atmos. Environ.*, **53**, 202–211, doi: 10.1016/j.atmosenv.2011.10.009.
- Friedl, M. A., D. K. McIver, J. C. F. Hodges, et al., 2002: Global land cover mapping from MODIS: Algorithms and early results. *Remote Sens. Environ.*, **83**, 287–302, doi: 10.1016/S0034-4257(02)00078-0.
- Grell, G. A., S. E. Peckham, R. Schmitz, et al., 2005: Fully coupled "online" chemistry within the WRF model. *Atmos. Environ.*, **39**, 6957–6975, doi: 10.1016/j.atmosenv.2005.04.027.
- Guenther, A., T. Karl, P. Harley, et al., 2006: Estimates of global terrestrial isoprene emissions using megan (model of emissions of gases and aerosols from nature). *Atmos. Chem. Phys.*, **6**, 3181–3210, doi: 10.5194/acp-6-3181-2006.
- He, K., 2012: Multi-resolution emission inventory for China (MEIC): Model framework and 1990–2010 anthropogenic emissions. AGU Fall Meeting. AGU Fall Meeting Abstracts. AGU, San Francisco, Calif., A32B-05.
- Hong, S. Y., J. Dudhia, and S. H. Chen, 2004: A revised approach to ice microphysical processes for the bulk parameterization of clouds and precipitation. *Mon. Wea. Rev.*, **132**, 103–120, doi: 10.1175/1520-0493(2004)132<0103:ARATIM>2.0.CO;2.
- Hong, S. Y., Y. Noh, and J. Dudhia, 2006: A new vertical diffusion package with an explicit treatment of entrainment processes. *Mon. Wea. Rev.*, **134**, 2318–2341, doi: 10.1175/MWR3199.1.
- Intergovernmental Panel on Climate Change (IPCC), 2007: *Climate Change 2007: The Physical Science Basis. Contribution of Working Group I to the Fourth Assessment Report of the Intergovernmental Panel on Climate Change*. Solomon, S., D. Qin, M. Manning, et al., Eds., Cambridge University Press, Cambridge, United Kingdom and New York, NY, USA, 1–87.
- Liu, H. N., L. Zhang, and J. Wu, 2010: A modeling study of the climate effects of sulfate and carbonaceous aerosols over China. *Adv. Atmos. Sci.*, **27**, 1276–1288, doi: 10.1007/s00376-010-9188-y.
- Mlawer, E. J., S. J. Taubman, P. D. Brown, et al., 1997: Radiative transfer for inhomogeneous atmospheres: RRTM, a validated correlated-k model for the longwave. *J. Geophys. Res. Atmos.*, **102**, 16663–16682, doi: 10.1029/97JD00237.
- Schell, B., I. J. Ackermann, H. Hass, et al., 2001: Modeling the formation of secondary organic aerosol within a comprehensive air quality model system. *J. Geophys. Res. Atmos.*, **106**, 28275–28293, doi: 10.1029/2001JD000384.
- Stockwell, W. R., P. Middleton, J. S. Chang, et al., 1990: The second generation regional acid deposition model chemical

- mechanism for regional air quality modeling. *J. Geophys. Res. Atmos.*, **95**, 16343–16367.
- Sun, K., H. N. Liu, A. J. Ding, et al., 2016: WRF-Chem simulation of a severe haze episode in the Yangtze River Delta, China. *Aerosol Air Quality Res.*, **16**, 1268–1283, doi: 10.4209/aaqr.2015.04.0248.
- Tao, M. H., L. F. Chen, X. Z. Xiong, et al., 2014: Formation process of the widespread extreme haze pollution over northern China in January 2013: Implications for regional air quality and climate. *Atmos. Environ.*, **98**, 417–425, doi: 10.1016/j.atmosenv.2014.09.026.
- Tie, X. X., and J. J. Cao, 2009: Aerosol pollution in China: Present and future impact on environment. *Particuology*, **7**, 426–431, doi: 10.1016/j.partic.2009.09.003.
- Wang, H., X. Y. Zhang, S. L. Gong, et al., 2013: The simulation study of the interaction between aerosols and heavy air pollution weather in East China. 19th International Conference on Nucleation and Atmospheric Aerosols, 24–28 June, Colorado State University, 499–502.
- Wang, X. Y., X. Z. Liang, W. M. Jiang, et al., 2010: WRF-Chem simulation of East Asian air quality: Sensitivity to temporal and vertical emissions distributions. *Atmos. Environ.*, **44**, 660–669, doi: 10.1016/j.atmosenv.2009.11.011.
- Wang, Z. F., J. Li, Z. Wang, et al., 2014: Modeling study of regional severe hazes over mid-eastern China in January 2013 and its implications on pollution prevention and control. *Sci. China Earth Sci.*, **57**, 3–13, doi: 10.1007/s11430-013-4793-0.
- Wendisch, M., S. Mertes, A. Ruggaber, et al., 2010: Vertical profiles of aerosol and radiation and the influence of a temperature inversion: Measurements and radiative transfer calculations. *J. Appl. Meteor.*, **35**, 1703–1715.
- Wild, O., X. Zhu, and M. J. Prather, 2000: Fast-J: Accurate simulation of in- and below-cloud photolysis in tropospheric chemical models. *J. Atmos. Chem.*, **37**, 245–282, doi: 10.1023/A:1006415919030.
- Yang, Y. L., J. H. Tan, J. R. Sun, et al., 2015: Synoptic effect of a heavy haze episode over North China. *Climatic Environ. Res.*, **20**, 555–570, doi: 10.3878/j.issn.1006-9585.2015.15018. (in Chinese)
- Zhang, B., Y. X. Wang, and J. M. Hao, 2015: Simulating aerosol–radiation–cloud feedbacks on meteorology and air quality over eastern China under severe haze conditions in winter. *Atmos. Chem. Phys.*, **15**, 2387–2404, doi: 10.5194/acp-15-2387-2015.
- Zhang, L., T. Wang, M. T. Lu, et al., 2015: On the severe haze in Beijing during January 2013: Unraveling the effects of meteorological anomalies with WRF-Chem. *Atmos. Environ.*, **104**, 11–21, doi: 10.1016/j.atmosenv.2015.01.001.
- Zhang, Y., X. Y. Wen, and C. J. Jang, 2010: Simulating chemistry–aerosol–cloud–radiation–climate feedbacks over the continental U. S. using the online-coupled Weather Research and Forecasting Model with chemistry (WRF/Chem). *Atmos. Environ.*, **44**, 3568–3582, doi: 10.1016/j.atmosenv.2010.05.056.
- Zhang, Y., X. Zhang, C. J. Cai, et al., 2014: Studying aerosol–cloud–climate interactions over East Asia using WRF/Chem. *Air Pollution Modeling and its Application XXIII*. Steyn, D., and R. Mathur, Eds., Cham, Springer International Publishing, 61–66.
- Zhao, C. F., and T. J. Garrett, 2015: Effects of Arctic haze on surface cloud radiative forcing. *Geophys. Res. Lett.*, **42**, 557–564, doi: 10.1002/2014GL062015.

Tech & Copy Editor: Zhirong CHEN  
Language Editor: Colin SMITH